Langmuir



Research Article

# Diffusioosmosis of Electrolyte Solutions in a Fine Capillary Tube

Huan J. Keh, and Hsien Chen Ma

*Langmuir*, **2007**, 23 (5), 2879-2886 • DOI: 10.1021/la062683n



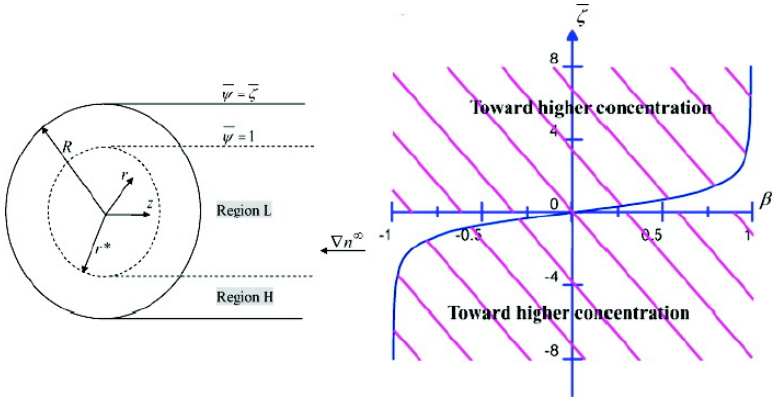


## More About This Article

Additional resources and features associated with this article are available within the HTML version:

- Supporting Information
- Links to the 1 articles that cite this article, as of the time of this article download
- Access to high resolution figures
- Links to articles and content related to this article
- Copyright permission to reproduce figures and/or text from this article

View the Full Text HTML

# Diffusioosmosis of Electrolyte Solutions in a Fine Capillary Tube

Huan J. Keh* and Hsien Chen Ma

*Department of Chemical Engineering, National Taiwan University, Taipei 10617, Taiwan, Republic of China*

*Received September 13, 2006. In Final Form: November 29, 2006*

A theoretical study is presented for the steady diffusioosmotic flow of an electrolyte solution in a fine capillary tube generated by a constant concentration gradient imposed in the axial direction. The capillary wall may have either a constant surface potential or a constant surface charge density of an arbitrary quantity. The electric double layer adjacent to the charged wall may have an arbitrary thickness, and its electrostatic potential distribution is determined by an analytical approximation to the solution of the Poisson−Boltzmann equation. Solving a modified Navier−Stokes equation with the constraint of no net electric current arising from the cocurrent diffusion, electric migration, and diffusioosmotic convection of the electrolyte ions, the macroscopic electric field and the fluid velocity along the axial direction induced by the imposed electrolyte concentration gradient are obtained semianalytically as a function of the radial position in a self-consistent way. The direction of the diffusioosmotic flow relative to the concentration gradient is determined by the combination of the zeta potential (or surface charge density) of the wall, the properties of the electrolyte solution, and other relevant factors. For a prescribed concentration gradient of an electrolyte, the magnitude of fluid velocity at a position in general increases with an increase in its distance from the capillary wall, but there are exceptions. The effect of the radial distribution of the induced tangential electric field and the relaxation effect due to ionic convection in the double layer on the diffusioosmotic flow are found to be very significant.

## 1. Introduction

The electrokinetic flows of an electrolyte solution in a small pore with a charged wall are of much fundamental and practical interest in various areas of science and engineering. Perhaps the most familiar example of electrokinetic flows is electroosmosis, which results from the interaction between an external tangential electric field and the electrical double layer adjacent to the charged wall. Problems of fluid flow caused by this well-known mechanism were studied extensively in the past.[1−12]

Another example of electrokinetic flows in a capillary pore, which is termed diffusioosmosis (also known as capillary osmosis[5,13]) and has caught less attention, involves a concentration gradient of the electrolyte along the capillary that interacts with the charged wall. Same as in the case of electroosmosis, the electrolyte−wall interaction in diffusioosmosis is electrostatic in nature and its range is the Debye screening length $\kappa^{-1}$ (defined right after eq 3). The fluid motion caused by diffusioosmosis has been analytically examined for flows near a plane wall[5,13−18] and inside a capillary pore.[19−23] Some experimental results and interesting applications concerning diffusioosmosis are also available in the literature.[24] Electrolyte solutions with a concentration gradient of order 100 kmol/m$^4$ (=1 M/cm) along solid surfaces with a zeta potential of order $kT/e$ (∼25 mV; $e$ is the charge of a proton, $k$ is the Boltzmann constant, and $T$ is the absolute temperature) can flow by diffusioosmosis at a velocity of several micrometers per second.

A tangential gradient of a dissociating electrolyte produces fluid flow along a charged solid surface by two mechanisms. The first involves the stresses developed by the tangential gradient of the excess pressure within the electric double layer (chemiosmotic effect), and the second is based on the macroscopic electric field that is generated because the tangential diffusive and convective fluxes of the two electrolyte ions are not equal (electroosmotic effect). Both mechanisms were considered to some extent in previous investigations for the diffusioosmotic flow.[13−23] In these studies, however, either the effect of lateral distributions of the counterions and co-ions (or of the electrostatic potential) on the local electric field induced by the imposed electrolyte concentration gradient in the tangential direction inside the double layer or the effect of the ionic convection on it caused by the diffusioosmotic flow was neglected. Moreover, the analyses concerning the diffusioosmotic flow in capillary tubes[22,23] are subject to the severe restriction that the zeta potential is sufficiently low (less than about 25 mV) for the Debye−Huckel approximation to be acceptable. In practical applications, however, zeta potentials as high as 100−200 mV are frequently encountered.

In this work we present a comprehensive analysis of the diffusioosmosis of an electrolyte solution with a constant

* To whom correspondence should be addressed. Fax: +886-2-23623040. E-mail: huan@ntu.edu.tw.

(1) Helmholtz, H. *Ann.* **1879**, *7*, 337.
(2) Smoluchowski, M. In *Handbuch der Elektrizitat und des Magnetismus*; Graetz, I., Ed.; Barth: Leipzig, 1921; Vol. 2, p 336.
(3) Burgreen, D.; Nakache, F. R. *J. Phys. Chem.* **1964**, *68*, 1084.
(4) Rice, C. L.; Whitehead, R. *J. Phys. Chem.* **1965**, *69*, 4017.
(5) Dukhin, S. S.; Derjaguin, B. V. In *Surface and Colloid Science*; Matijevic, E., Ed.; Wiley: New York, 1974; Vol. 7.
(6) Levine, S.; Marriott, J. R.; Neale, G.; Epstein, N. *J. Colloid Interface Sci.* **1975**, *52*, 136.
(7) Ohshima, H.; Kondo, T. *J. Colloid Interface Sci.* **1990**, *135*, 443.
(8) Masliyah, J. H. *Electrokinetic Transport Phenomena*; AOSTRA: Edmonton, Alberta, Canada, 1994.
(9) Yang, C.; Li, D. *J. Colloid Interface Sci.* **1997**, *194*, 95.
(10) Szymczyk, A.; Aoubiza, B.; Fievet, P.; Pagetti, J. *J. Colloid Interface Sci.* **1999**, *216*, 285.
(11) Keh, H. J.; Tseng, H. C. *J. Colloid Interface Sci.* **2001**, *242*, 450.
(12) Keh, H. J.; Ding, J. M. *J. Colloid Interface Sci.* **2003**, *263*, 645.
(13) Derjaguin, B. V.; Dukhin, S. S.; Korotkova, A. A. *Kolloid. Zh.* **1961**, *23*, 53.
(14) Prieve, D. C.; Anderson, J. L.; Ebel, J. P.; Lowell, M. E. *J. Fluid Mech.* **1984**, *148*, 247.
(15) Anderson, J. L. *Annu. Rev. Fluid Mech.* **1989**, *21*, 61.
(16) Pawar, Y.; Solomentsev, Y. E.; Anderson, J. L. *J. Colloid Interface Sci.* **1993**, *155*, 488.
(17) Keh, H. J.; Chen, S. B. *Langmuir* **1993**, *9*, 1142.
(18) Keh, H. J.; Ma, H. C. *Langmuir* **2005**, *21*, 5461.
(19) Fair, J. C.; Osterle, J. F. *J. Chem. Phys.* **1971**, *54*, 3007.
(20) Sasidhar, V.; Ruckenstein, E. *J. Colloid Interface Sci.* **1982**, *85*, 332.
(21) Westermann-Clark, G. B.; Anderson, J. L. *J. Electrochem. Soc.* **1983**, *130*, 839.
(22) Keh, H. J.; Wu, J. H. *Langmuir* **2001**, *17*, 4216.
(23) Keh, H. J.; Ma, H. C. *Colloids Surf., A* **2004**, *233*, 87.
(24) Dukhin, S. S. *Adv. Colloid Interface Sci.* **1993**, *44*, 1.

10.1021/la062683n CCC: $37.00 
Published on Web 01/30/2007

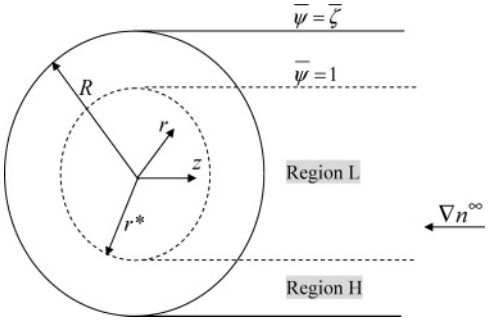


**Figure 1.** Geometrical sketch for the diffusioosmosis in a capillary tube due to an axially applied concentration gradient of electrolyte.

prescribed concentration gradient in the axial direction of a narrow capillary tube. The zeta potential or surface charge density of the capillary wall is assumed to be uniform, but no assumption is made concerning the magnitude of the zeta potential or the thickness of the double layer, and both the radial distribution of the induced axial electric field and the effect of the ionic convection on it are allowed. The Poisson−Boltzmann equation governing the electrostatic potential within the capillary is solved by an analytical approximation, which has been shown to yield results differing only slightly from the exact numerical solution.[6,25] Semianalytical results for the diffusioosmotic velocity profile are obtained for various cases. These results show that the effect of the deviation of the induced axial electric field in the double layer from its bulk-phase quantity and the effect of the ionic convection on the diffusioosmotic velocity of the fluid are very significant in most practical situations, even for the case of a very thin double layer.

## 2. Electrostatic Potential Distribution

In this section, we consider the radial distribution of the electrostatic potential in the fluid solution of a symmetrically charged electrolyte of valence $Z$ (where $Z$ is a positive integer) undergoing diffusioosmosis in a straight capillary tube of radius $R$ and length $L$ with $R \ll L$, as illustrated in Figure 1, at the steady state. The discrete nature of the surface charges, which are uniformly distributed over the capillary wall, is ignored. The applied electrolyte concentration gradient $\nabla n^{\infty}$ is a constant along the axial ($z$) direction in the capillary, where $n^{\infty}(z)$ is the linear concentration (number density) distribution of the electrolyte in the bulk solution phase in equilibrium with the fluid inside the capillary. The electrolyte ions can diffuse freely in the capillary, so there exists no regular osmotic flow of the solvent. The end effects are neglected. It is assumed that $n^{\infty}$ is only slightly nonuniform such that $L|\nabla n^{\infty}|/n^{\infty}(0) \ll 1$, where $z = 0$ is set at the midpoint through the capillary. Thus, the variation of the electrostatic potential (excluding the macroscopic electric field induced by the electrolyte gradient, which will be discussed in section 3) and ionic concentrations in the electric double layer adjacent to the capillary wall with the axial position can be neglected in comparison with their corresponding quantities at $z = 0$.

If $\psi(r)$ represents the electrostatic potential at a point with distance $r$ from the axis of the capillary tube relative to that in the bulk solution, and $n_+(r,z)$ and $n_-(r,z)$ denote the local concentrations of the cations and anions, respectively, then the Poisson equation gives

$$\frac{1}{r}\frac{\mathrm{d}}{\mathrm{d}r}\left(r\frac{\mathrm{d}\psi}{\mathrm{d}r}\right) = -\frac{4\pi Ze}{\epsilon}[n_+(r,0) - n_-(r,0)] \qquad (1)$$

In this equation, $\epsilon = 4\pi\epsilon_0\epsilon_r$, where $\epsilon_r$ is the relative permittivity of the electrolyte solution and $\epsilon_0$ is the permittivity of a vacuum.

The local ionic concentrations can also be related to the electrostatic potential by the Boltzmann equation

$$n_{\pm} = n^{\infty}\exp(\mp\bar{\psi}) \qquad (2)$$

where $\bar{\psi} = Ze\psi/kT$ is the dimensionless potential profile. Substitution of eq 2 into eq 1 results in the well-known Poisson−Boltzmann equation

$$\frac{1}{r}\frac{\mathrm{d}}{\mathrm{d}r}\left(r\frac{\mathrm{d}\bar{\psi}}{\mathrm{d}r}\right) = \kappa^2\sinh\bar{\psi} \qquad (3)$$

where $\kappa = [8\pi(Ze)^2n^{\infty}(0)/\epsilon kT]^{1/2}$ is the Debye screening parameter.

**2.1. The Case of Constant Surface Potential.** For the case of constant surface potential, the boundary conditions for $\psi$ are

$$r = 0: \qquad \frac{\mathrm{d}\bar{\psi}}{\mathrm{d}r} = 0 \qquad (4a)$$

$$r = R: \qquad \bar{\psi} = \bar{\zeta} \qquad (4b)$$

where the constant $\bar{\zeta} = Ze\zeta/kT$ is the dimensionless zeta potential at the shear plane of the capillary wall adjacent to the electrolyte solution having a uniform bulk concentration $n^{\infty}(0)$.

Since there is no simple analytical solution of eq 3 available for the case of cylindrical symmetry, we follow a previous approach[6,25] and use an approximation to provide a good representation of $\sinh\bar{\psi}$ throughout the range $\bar{\psi} \geq 0$

$$\sinh\bar{\psi} = \bar{\psi} \qquad \text{if} \quad 0 \leq \bar{\psi} < 1 \qquad (5a)$$

$$\sinh\bar{\psi} = \frac{1}{2}e^{\bar{\psi}} \qquad \text{if} \quad \bar{\psi} > 1 \qquad (5b)$$

and replace eq 3 by a pair of equations

$$\frac{1}{r}\frac{\mathrm{d}}{\mathrm{d}r}\left(r\frac{\mathrm{d}\bar{\psi}_{\mathrm{L}}}{\mathrm{d}r}\right) = \kappa^2\bar{\psi}_{\mathrm{L}} \qquad \text{if} \quad 0 \leq r \leq r^* \qquad (6a)$$

$$\frac{1}{r}\frac{\mathrm{d}}{\mathrm{d}r}\left(r\frac{\mathrm{d}\bar{\psi}_{\mathrm{H}}}{\mathrm{d}r}\right) = \frac{1}{2}\kappa^2e^{\bar{\psi}} \qquad \text{if} \quad r^* \leq r \leq R \qquad (6b)$$

Only the positive values of $\bar{\psi}$ are considered here without the loss of generality.

In this approach, we have divided the capillary into two hypothetical concentric regions such that $\bar{\psi} = 1$ ( $\sinh\bar{\psi} = 1.175$ and $e^{\bar{\psi}}/2 = 1.359$) at their junction $r = r^*$, where the subscripts L and H designate the inner (or low potential) and outer (or high potential) regions, respectively, as shown in Figure 1. If $\bar{\zeta} \leq 1$, then region L comprises the whole of the capillary tube. If $\bar{\psi}(0) \geq 1$, then region H occupies the whole tube. In other cases, eq 6 is subject to eq 4 and the additional boundary conditions

$$r = r^*: \qquad \bar{\psi}_{\mathrm{L}} = \bar{\psi}_{\mathrm{H}} = 1 \qquad (7a)$$

$$\frac{\mathrm{d}\bar{\psi}_{\mathrm{L}}}{\mathrm{d}r} = \frac{\mathrm{d}\bar{\psi}_{\mathrm{H}}}{\mathrm{d}r} \qquad (7b)$$

which together ensure that the calculated $\bar{\psi}(r)$ profile, albeit approximate, will be a smooth continuous function in the neighborhood of $r = r^*$.

The relation among the dimensionless parameters $\kappa r^*$, $\bar{\zeta}$, and $\kappa R$ is displayed in Figure 2 and the analytical solutions for $\bar{\psi}_{\mathrm{L}}(r)$ and $\bar{\psi}_{\mathrm{H}}(r)$ are outlined below in terms of several subdomains.

(25) Philip, J. R.; Wooding, R. A. *J. Chem. Phys.* **1970**, *52*, 953.

In subdomain I ( $\bar{\zeta} \le 1$), the low potential region fills the capillary entirely, and the electrostatic potential distribution is

$$\bar{\psi}_{\mathrm{L}}(r) = \bar{\zeta}\frac{I_0(\kappa r)}{I_0(\kappa R)} \qquad \text{for} \quad 0 \le r \le R \tag{8}$$

where $I_n$ is the modified Bessel function of the first kind of order $n$. As expected, Figure 2 illustrates that $r^* = R$ as $\bar{\zeta} = 1$.

In subdomain IIA ( $r^* > r_0^*$, where $r_0^*$ is a critical value of $r^*$ used to provide ranges for the subdomains), the solution of eqs 6, 7, and 4 results in

$$\bar{\psi}_{\mathrm{L}}(r) = \frac{I_0(\kappa r)}{I_0(\kappa r^*)} \quad \text{for} \quad 0 \le r \le r^* \tag{9a}$$

$$\bar{\psi}_{\mathrm{H}}(r) = \ln\left\{\frac{-C}{(\kappa r)^2 \cos^2[\cos^{-1}\sqrt{-C/(\kappa r^*)^2 e} + \sqrt{-C/4}\ln(r/r^*)]}\right\} \tag{9b}$$

for $r^* \le r \le R$

where $C$ is an integration constant dependent on the parameter $\kappa r^*$

$$C = \left[2 + \kappa r^* \frac{I_1(\kappa r^*)}{I_0(\kappa r^*)}\right]^2 - (\kappa r^*)^2 e \tag{10}$$

The above equation gives $C < 0$ (and a meaningful solution in eq 9b) for $r^* > r_0^*$ and $C = 0$ at $r^* = r_0^*$ (the junction of subdomains IIA and IIB), where $\kappa r_0^* = 2.15852$; in the latter case eq 9b becomes

$$\bar{\psi}_{\mathrm{H}}(r) = -2\ln\left(\frac{r}{\sqrt{e}r_0^*} - \frac{\kappa r}{2}\ln\frac{r}{r_0^*}\right) \tag{11}$$

for $r^* \le r \le R$

In the subdomain IIB ( $0 < r^* < r_0^*$ and $0 < C < 4$), $\bar{\psi}_{\mathrm{L}}$ is also given by eq 9a, while eq 9b is replaced by

$$\bar{\psi}_{\mathrm{H}}(r) = \ln\left\{\frac{4AC(r/r^*)^{\sqrt{C}}}{(\kappa r)^2[1 - A(r/r^*)^{\sqrt{C}}]^2}\right\}$$

for $r^* \le r \le R$ (12)

where

$$A = \frac{\sqrt{C + (\kappa r^*)^2 e} - \sqrt{C}}{\sqrt{C + (\kappa r^*)^2 e} + \sqrt{C}} \tag{13}$$

In the subdomain III ($r^* = 0$, $C = 4$, and $\bar{\psi}_{\mathrm{H}}(0) \ge 1$), the region of the potential $\bar{\psi}_{\mathrm{H}}$ fills the capillary entirely, and

$$\bar{\psi}_{\mathrm{H}}(r) = \bar{\psi}_{\mathrm{H}}(0) - 2\ln\left[1 - \frac{(\kappa r)^2}{16}e^{\bar{\psi}_{\mathrm{H}}(0)}\right]$$

for $0 \le r \le R$ (14)

Here, the quantity $\bar{\psi}_{\mathrm{H}}(0)$ can be determined as a function of the parameters $\bar{\zeta}$ and $\kappa R$ from the above equation setting $r = R$ and $\bar{\psi}_{\mathrm{H}}(R) = \bar{\zeta}$.

Usually an analytical solution of the Poisson−Boltzmann equation in the form of eq 3 is obtained either for a small zeta potential $\bar{\zeta}$ or for a large electrokinetic radius $\kappa R$. An advantage of the above analysis is the method to find the potential distribution $\bar{\psi}$ for any values of $\bar{\zeta}$ and $\kappa R$.

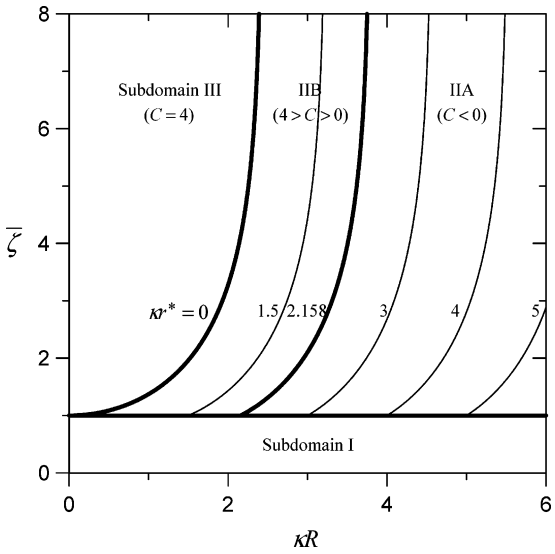


**Figure 2.** Map showing the relation among the dimensionless parameters $\kappa r^*$, $\bar{\zeta}$, and $\kappa R$ and displaying the fundamental subdomains for the solution of $\bar{\psi}(r)$.

**2.2. The Case of Constant Surface Charge Density.** If the constant surface charge density $\sigma$, instead of the surface potential $\zeta$, is known at the capillary wall, the boundary condition specified by eq 4b should be replaced by the Gauss condition

$$r = R: \qquad \frac{\mathrm{d}\psi}{\mathrm{d}r} = \frac{4\pi\sigma}{\epsilon} \tag{15}$$

The solutions for $\psi$ given by eqs 8−14 still hold for this condition, with the connection between $\zeta$ and $\sigma$ for an arbitrary value of $\kappa R$ as

$$\bar{\zeta} = \frac{\bar{\sigma}}{\kappa R}\frac{I_0(\kappa R)}{I_1(\kappa R)} \qquad \text{if} \quad \bar{\zeta} \le 1 \tag{16a}$$

$$\bar{\zeta} = \ln\frac{(\bar{\sigma} + 2)^2 - C}{(\kappa R)^2} \qquad \text{otherwise} \tag{16b}$$

where $\bar{\sigma} = 4\pi RZe\sigma/\epsilon kT$ is the dimensionless surface charge density. Equation 16 indicates that, for a given electrolyte solution in a capillary tube with a specified radius, $\sigma$ increases (almost linearly) with an increase in $\kappa$ or $[n^\infty(0)]^{1/2}$ for the case of constant surface potential, and $\zeta$ decreases with an increase in $\kappa$ or $[n^\infty(0)]^{1/2}$ for the case of constant surface charge density.

## 3. Induced Electric Field Distribution

The ionic concentrations $n_+$ and $n_-$ in the fluid undergoing diffusioosmosis in the capillary are not uniform in both axial ($z$) and radial ($r$) directions; hence their prescribed gradients in the axial direction can give rise to a "diffusion current" distribution on a cross section of the capillary. To prevent a continuous separation of the counterions and co-ions, an electric field distribution along the axial direction arises spontaneously in the electrolyte solution to produce another electric current distribution which exactly balances the diffusion current.[13−18] This induced electric field generates an electroosmotic flow of the fluid in the capillary, in addition to the chemiosmotic flow caused by the prescribed electrolyte gradient directly. Both the chemiosmotic and the electroosmotic flows also generate an electric current distribution by the ionic convection (known as the relaxation

effect), and alternately, this secondary "convection current" again needs to be balanced by the electric current contributed from the induced electric field.

The total flux of either ionic species can be expressed as the general form

$$\mathbf{J}_{\pm} = -D_{\pm}\left[\nabla n_{\pm} \pm \frac{Ze}{kT} n_{\pm}(\nabla\psi - \mathbf{E})\right] + n_{\pm}\mathbf{u} \qquad (17)$$

where $\mathbf{u} = u(r)\mathbf{e}_z$ is the fluid velocity in the axial direction of decreasing electrolyte concentration (i.e., $\mathbf{e}_z$ is the unit vector in the direction of $-\nabla n^{\infty}$), $D_+$ and $D_-$ are the diffusion coefficients of the cations and anions, respectively, $\mathbf{E} = E(r)\mathbf{e}_z$ is the macroscopic electric field induced by the prescribed concentration gradient of the electrolyte, and the principle of superposition for the electric potential is used. To have no net electric current arising from the cocurrent diffusion, electric migration, and diffusioosmotic convection of the cations and anions, one must require that $\mathbf{J}_+ = \mathbf{J}_- = \mathbf{J}$ (obviously, the radial component of $\mathbf{J}$ vanishes and the ionic fluxes induced by $\nabla\psi$ in eq 17 are balanced by the radial components of the diffusive ionic fluxes as required by the Boltzmann distribution given by eq 2).

Applying the constraint $\mathbf{J}_+ = \mathbf{J}_-$ to eq 17, we obtain[26]

$$\mathbf{E} = \frac{kT}{Ze}\frac{\nabla n^{\infty}}{n^{\infty}(0)}\left[\frac{(1+\beta)e^{-\bar{\psi}} - (1-\beta)e^{\bar{\psi}}}{(1+\beta)e^{-\bar{\psi}} + (1-\beta)e^{\bar{\psi}}} + \frac{\mathrm{Pe}\sinh\bar{\psi}}{(1+\beta)e^{-\bar{\psi}} + (1-\beta)e^{\bar{\psi}}}\frac{u}{U^*}\right] \qquad (18)$$

where

$$U^* = \frac{\epsilon|\nabla n^{\infty}|}{4\pi\eta n^{\infty}(0)}\left(\frac{kT}{Ze}\right)^2 = \frac{2kT}{\eta\kappa^2}|\nabla n^{\infty}| \qquad (19)$$

which is a characteristic value of the diffusioosmotic velocity

$$\beta = \frac{D_+ - D_-}{D_+ + D_-} \qquad (20)$$

$$\mathrm{Pe} = \frac{4n^{\infty}(0)U^*}{(D_+ + D_-)|\nabla n^{\infty}|} = \frac{8n^{\infty}(0)kT}{(D_+ + D_-)\eta\kappa^2} \qquad (21)$$

and $\eta$ is the fluid viscosity. As it is defined by eq 20, $-1 \le \beta \le 1$, with the upper and lower bounds occurring as $D_-/D_+ \to 0$ and $\infty$, respectively.

Typical values of the physical quantities in eqs 18−21 are $U^* = 10^{-5}$ m/s, $D_{\pm} = 10^{-9}$ m$^2$/s, $n^{\infty}(0)/|\nabla n^{\infty}| = 10^{-4}$ m, and Pe of order unity. The induced electric field $\mathbf{E}$ given by eq 18 in a self-consistent way depends on the local electrostatic potential $\psi$ and fluid velocity $u$. It indicates that $\mathbf{E}$ is collinear with and proportional to the axially imposed electrolyte gradient $\nabla n^{\infty}$.

If we consider the situation that $\kappa R \gg 1$, then, at a position $r \ll R$, $\psi \to 0$ and eq 18 for the induced electric field caused by the imposed electrolyte concentration gradient reduces to its bulk-phase quantity

$$\mathbf{E}^{\infty} = \frac{kT}{Ze}\frac{\beta\nabla n^{\infty}}{n^{\infty}(0)} \qquad (22)$$

For the special case of an uncharged wall ($\zeta = 0$), $\mathbf{E}$ at any location $r$ is also identical to this bulk-phase quantity. Note that $\mathbf{E}^{\infty}$ is linearly proportional to the parameter $\beta$, but $\mathbf{E}(r)$ is not necessarily to vanish if $\beta = 0$, even as Pe = 0, as shown in eq 18.

(26) Ma, H. C.; Keh, H. J. *J. Colloid Interface Sci.* **2006**, *298*, 476.

## 4. Fluid Velocity Distribution

We now consider the steady diffusioosmotic flow of a symmetric electrolyte solution in a capillary tube under the influence of a constant concentration gradient of the electrolyte prescribed axially. The momentum balances on the incompressible and Newtonian fluid in the $r$ and $z$ directions give

$$\frac{\partial p}{\partial r} + Ze(n_+ - n_-)\frac{\mathrm{d}\psi}{\mathrm{d}r} = 0 \qquad (23a)$$

$$\frac{\eta}{r}\frac{\mathrm{d}}{\mathrm{d}r}\left(r\frac{\mathrm{d}u}{\mathrm{d}r}\right) = \frac{\partial p}{\partial z} - Ze(n_+ - n_-)E \qquad (23b)$$

where $p(r,z)$ is the dynamic pressure distribution. The boundary conditions for $u$ at the axis and at the no-slip wall of the capillary tube are

$$r = 0: \qquad \frac{\mathrm{d}u}{\mathrm{d}r} = 0 \qquad (24a)$$

$$r = R: \qquad u = 0 \qquad (24b)$$

After the substitution of eq 2 into eq 23a based on the assumption that the equilibrium ionic distributions are not affected by the net electrolyte flux $\mathbf{J}$, which is warranted if $|\nabla n^{\infty}|/\kappa n^{\infty}(0) \ll 1$, the pressure distribution can be determined as

$$p = p_0 + 2kTn^{\infty}(z)\{\cosh(\bar{\psi}) - \cosh[\bar{\psi}(0)]\} \qquad (25)$$

Here, $p_0$ is the pressure on the axis of the capillary tube, which is a constant in the absence of the applied pressure gradient, and the electric potential distribution $\psi(r)$ is given by eqs 8−14.

Substituting the ionic concentration distributions of eq 2 and the pressure profile of eq 25 into eq 23b and then performing the integration with respect to $r$ twice subject to the boundary conditions in eq 24, we obtain

$$\frac{u}{U^*} = (\kappa R)^2\int_1^{r/R}\frac{R}{r}\int_0^{r/R}\frac{r}{R}\left[\cosh\bar{\psi} - \cosh\bar{\psi}(0) + \frac{Zen^{\infty}(0)}{kT|\nabla n^{\infty}|}E\sinh\bar{\psi}\right]\mathrm{d}\left(\frac{r}{R}\right)\mathrm{d}\left(\frac{r}{R}\right) \qquad (26)$$

After the substitution of eq 26 for $u$ and eqs 8−14 for $\bar{\psi}$ into eq 18, the induced electric field distribution $E$ can be numerically solved as a function of the dimensionless parameters $\kappa R$, $\bar{\zeta}$, $\beta$, and Pe. With the known results of $\bar{\psi}$ and $E$, the diffusioosmotic velocity distribution of the electrolyte solution as a function of $\kappa R$, $\bar{\zeta}$, $\beta$, and Pe can be determined from eq 26 with the numerical integrations. As expected, eq 26 yields $u/U^* = 0$ (since $\bar{\psi} = 0$) everywhere if $\zeta = 0$. It is understood that, for given values of $\kappa R$, Pe, and $r/R$, the quantity $u/U^*$ with specified values $-\bar{\zeta}$ and $\beta$ is equal to that with the values $\bar{\zeta}$ and $-\beta$.

## 5. Results and Discussion

**5.1. Method of the Numerical Calculation.** The distribution of the macroscopic electric field $E(r)$ induced by the concentration gradient of a symmetric electrolyte prescribed axially in a capillary tube can be numerically determined after substituting the fluid velocity $u(r)/U^*$ in the form of eq 26 and the electric potential $\bar{\psi}(r)$ calculated from eqs 8−14 into eq 18. A simple method of this numerical calculation is to make an initial guess of the fluid velocity distribution $u_1(r/R)/U^*$ for a given combination of the

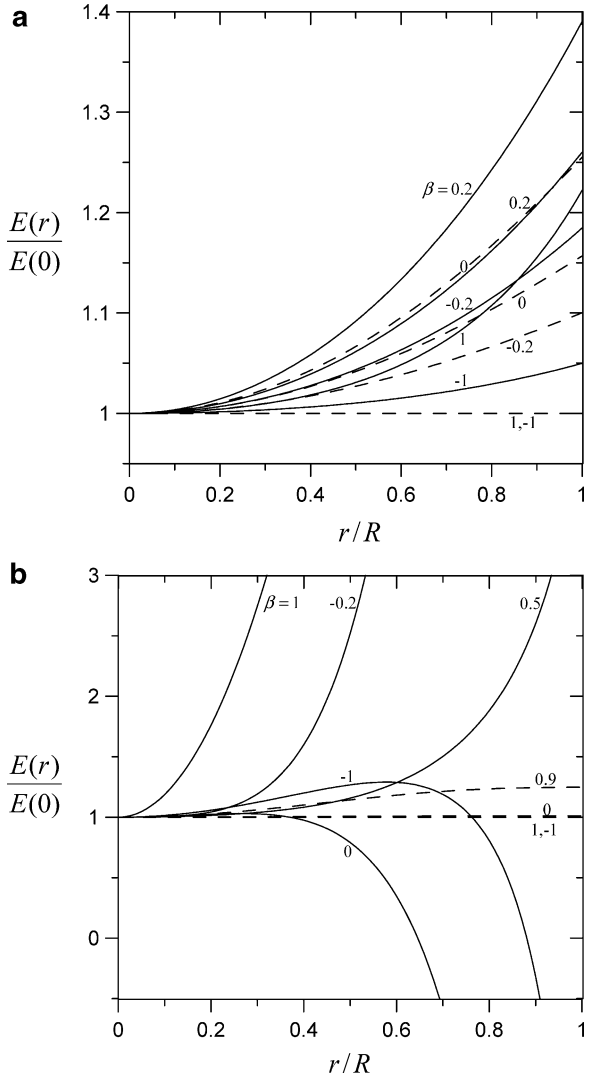


**Figure 3.** Plots of the normalized electric field induced by an electrolyte gradient in the axial direction of a capillary tube versus the dimensionless coordinate $r/R$ for the case of $\kappa R = 1$ with various values of the parameter $\beta$: (a) $\bar{\zeta} = 1$; (b) $\bar{\zeta} = 6$. The solid curves represent the case Pe = 1 and the dashed curves denote the case Pe = 0.

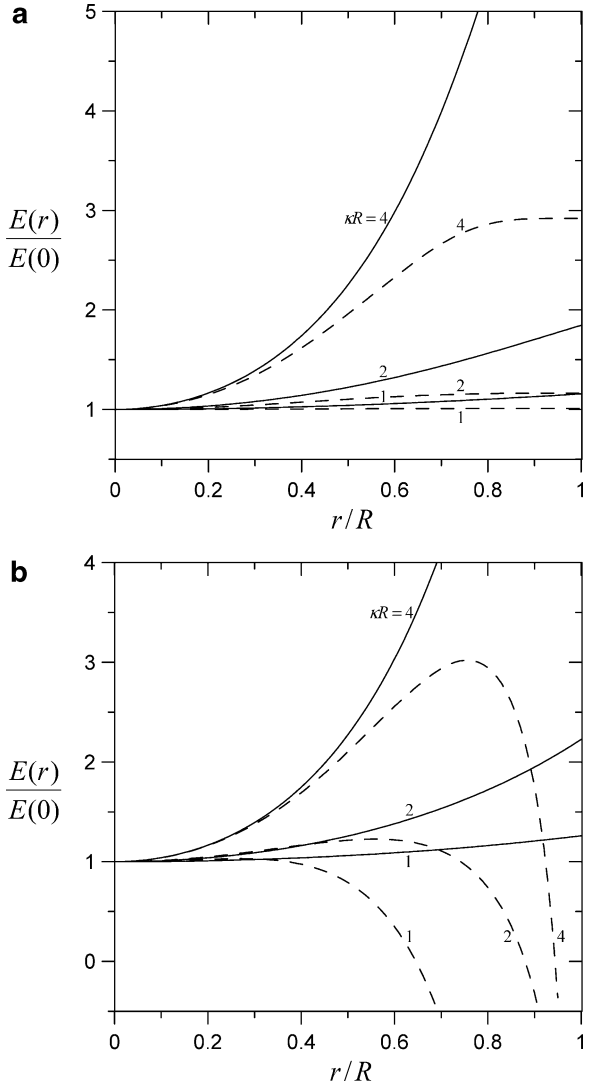


**Figure 4.** Plots of the normalized electric field induced by an electrolyte gradient in the axial direction of a capillary tube versus the dimensionless coordinate $r/R$ for the case of $\beta = 0$ with various values of the parameter $\kappa R$: (a) Pe = 0; (b) Pe = 1. The solid curves represent the case $\bar{\zeta} = 1$, and the dashed curves denote the case $\bar{\zeta} = 6$.

dimensionless parameters $\bar{\zeta}$, $\beta$, Pe, and $\kappa R$, and to obtain the resulting induced electric field $E_1(r/R)$ from eq 18. Then, the next result of the velocity distribution $u_2(r/R)/U^*$ can be determined from the double integral involving $E_1(r/R)$ in eq 26. If the difference between $u_2(r/R)$ and $u_1(r/R)$ is beyond the tolerable error, then $u_2(r/R)/U^*$ is used in eq 18 to obtain $E_2(r/R)$, and the same procedure will be repeated until an acceptable result of the velocity distribution is obtained.

**5.2. Induced Electric Field Distribution.** The induced electric field caused by the axially prescribed electrolyte gradient in the capillary tube normalized by its quantity at the axis, $E(0)$, as a function of the normalized coordinate $r/R$ is plotted in Figures 3 and 4 for several values of the parameters $\bar{\zeta}$, $\beta$, Pe, and $\kappa R$. Note that each curve with specified values of $-\bar{\zeta}$ and $\beta$ in the figures would be identical to that with the values $\bar{\zeta}$ and $-\beta$. As expected, the magnitude of the normalized induced electric field in general is a sensitive function of $r/R$ and can deviate much from its bulk-phase value. This fact plays an important role on the electroosmotic contribution to the fluid velocity.[23]

When Pe = 0, the effect of the ionic convection on the induced electric field is not involved, as indicated in eq 18. In this case, $E(r)/E(0)$ is positive and its value increases with an increase in $r/R$ from unity at the axis of the tube to a maximum at the capillary wall, increases with an increase in $\kappa R$, decreases with an increase in $|\bar{\zeta}|$, equals unity in the limits $\beta\zeta/|\zeta| = \pm 1$, and increases with an increase in $\beta\zeta/|\zeta|$ if it is not too close to unity (depending on the value of $\kappa R$), for an otherwise specified condition.

On the other hand, when the value of Pe is finite, the value of $E(r)/E(0)$ is larger than that for the case of Pe = 0 if the magnitude of $\bar{\zeta}$ is small (depending on the values of $\kappa R$ and $\beta$), but it may not be a monotonic function of $r/R$ and may become negative if the magnitude of $\bar{\zeta}$ is large. In general, the effect of the electrolyte convection on the local induced electric field in the electric double layer adjacent to the capillary wall can be quite significant, not only quantitatively but also qualitatively, even for the case of low zeta potential at the wall.

**5.3. Fluid Velocity Distribution.** The dimensionless diffusioosmotic velocity distribution $u(r)/U^*$ of an electrolyte solution in a capillary tube numerically calculated using eq 26 with the known distributions of $\bar{\psi}$ and $E$ is plotted in Figures 5 and 6 for several values of the parameters $\bar{\zeta}$, $\beta$, Pe, and $\kappa R$. This diffusioosmotic velocity can be either positive or negative and

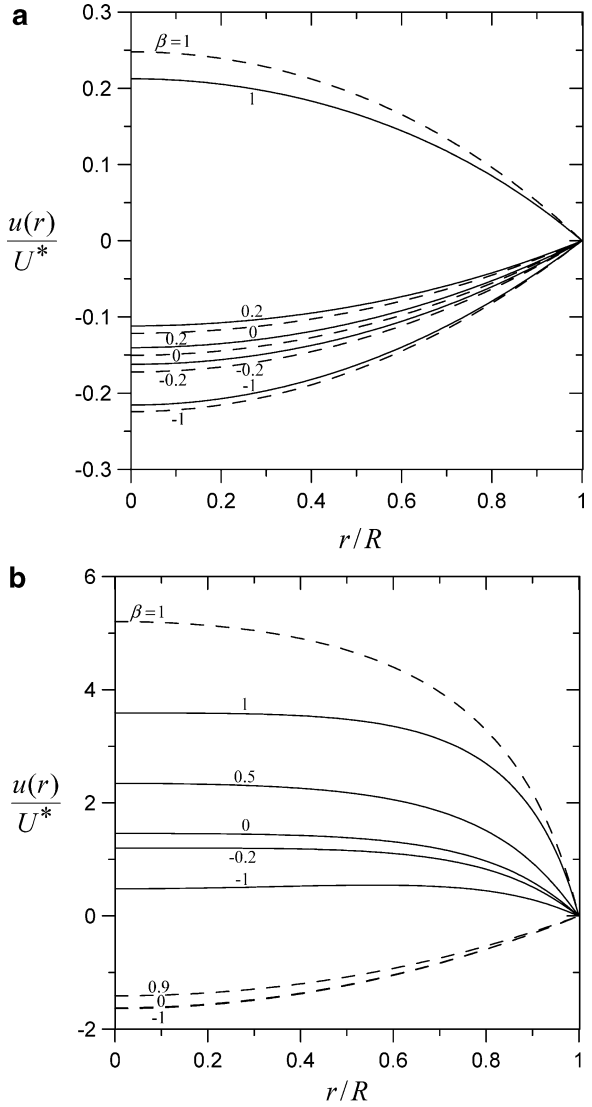


**Figure 5.** Plots of the normalized diffusioosmotic velocity in a capillary tube versus the dimensionless coordinate $r/R$ for the case of $\kappa R = 1$ with various values of the parameter $\beta$: (a) $\bar{\zeta} = 1$; (b) $\bar{\zeta} = 6$. The solid curves represent the case Pe = 1 and the dashed curves denote the case Pe = 0.

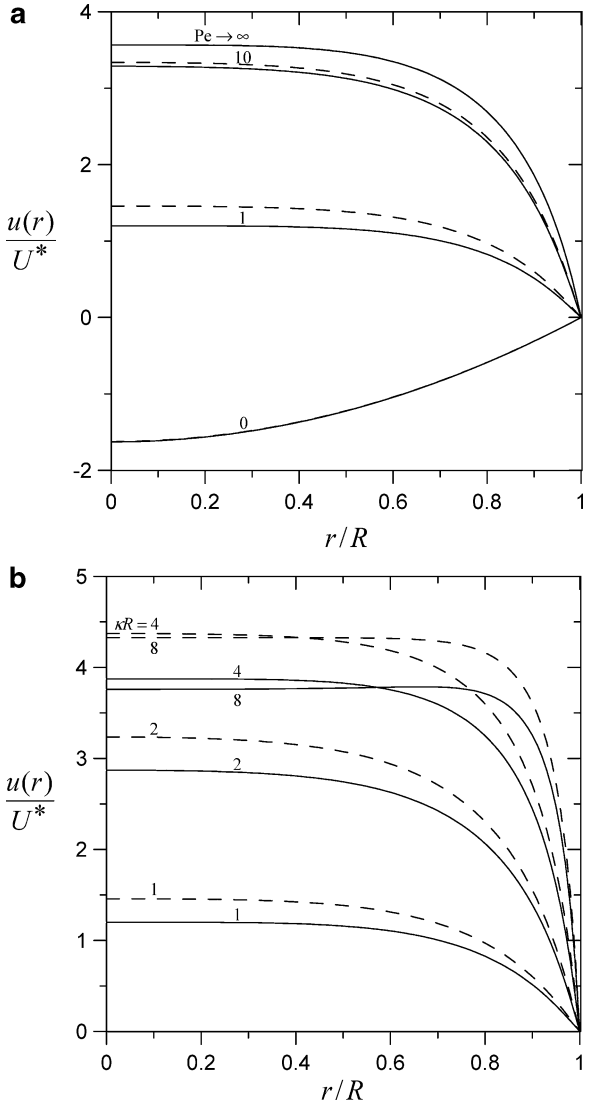


**Figure 6.** Plots of the normalized diffusioosmotic velocity in a capillary tube versus the dimensionless coordinate $r/R$ for the case of $\bar{\zeta} = 6$: (a) $\kappa R = 1$; (b) Pe = 1. The solid curves represent the case $\beta = -0.2$, and the dashed curves denote the case $\beta = 0$.

is a monotonic increasing function of $\beta\zeta/|\zeta|$. In general, the magnitude of $u/U^*$ decreases monotonically with an increase in the normalized coordinate $r/R$ (there are exceptions), but it is not necessarily a monotonic function of $\kappa R$ for given values of $\beta$, Pe, and $r/R$.

When Pe = 0 and $\beta\zeta/|\zeta|$ is not too close to unity, $u$ is negative, meaning that the diffusioosmotic flow is in the direction of increasing electrolyte concentration, and the magnitude of $u/U^*$ increases with an increase in $|\bar{\zeta}|$ and with a decrease in $\beta\zeta/|\zeta|$, for an otherwise specified condition. When Pe = 0 and $\beta\zeta/|\zeta|$ approaches unity, the fluid flows against the electrolyte concentration gradient ($u$ is positive) and $u/U^*$ is a monotonic increasing function of $|\bar{\zeta}|$.

When the value of Pe is finite, the dependence of $u$ on $r/R$ is similar to that for the case of Pe = 0 if the value of $|\bar{\zeta}|$ is small, but $u$ can be positive for any given value of $\beta$ if the value of $|\bar{\zeta}|$ is large. In general, the value of $u/U^*$ increases monotonically and remarkably with an increase in the value of Pe (the relaxation effect due to ionic convection on the diffusioosmotic flow is very significant) for specified values of $\kappa R$, $\bar{\zeta}$, and $\beta$ except for the situation that the value of $\beta\zeta/|\zeta|$ is close to unity. In the limit of Pe → ∞, $u/U^*$ is finite. Note that the case with Pe ≥ 10, which are not likely to exist in practice, is exhibited in Figure 6a for the sake of numerical comparison.

**5.4. Fluid Velocity at the Axis of the Tube.** In Figure 7, the normalized diffusioosmotic velocity $u(0)/U^*$ of the electrolyte solution at the axis of the capillary tube is plotted versus the parameters $\kappa R$ and $\bar{\zeta}$ at specified values of Pe and $\beta$. Maps showing the direction of this velocity for a typical value of $\kappa R$ are also drawn in Figure 9. The dependence of $u(0)/U^*$ on $\bar{\zeta}$, $\beta$, $\kappa R$, and Pe is quite similar to that of $u/U^*$ for a given value of $r/R$, and it is not necessarily a monotonic function of $\kappa R$ for given values of $\beta$ and Pe.

When Pe = 0 and the product of $\zeta$ and $\beta$ is negative (inside the second and fourth quadrants in Figure 8a), $u(0)$ is negative and the electrolyte solution flows toward higher concentration. When Pe = 0 and the product of $\zeta$ and $\beta$ is positive (inside the first and third quadrants in Figure 8a), the diffusioosmotic velocity $u(0)$ may reverse its direction from against the concentration gradient to along with it as $|\bar{\zeta}|$ increases not much from zero for all practical cases of $\beta$ (in addition to a reversal occurring at $\bar{\zeta} = 0$), or as $|\beta|$ decreases from 1 to 0 for a small magnitude of $\bar{\zeta}$.

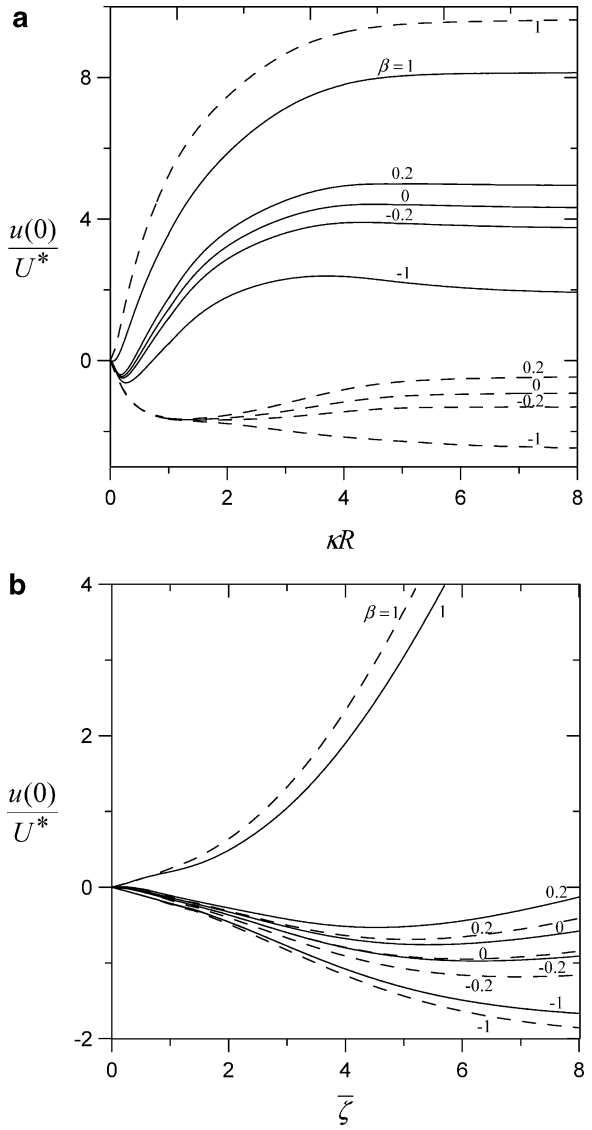


**Figure 7.** The normalized diffusioosmotic velocity at the axis of a capillary tube for various values of the parameter $\beta$: (a) plots vs $\kappa R$ for the case of $\bar{\zeta} = 6$; (b) plots vs $\bar{\zeta}$ for the case of $\kappa R = 1$. The solid curves represent the case Pe = 1 and the dashed curves denote the case Pe = 0.

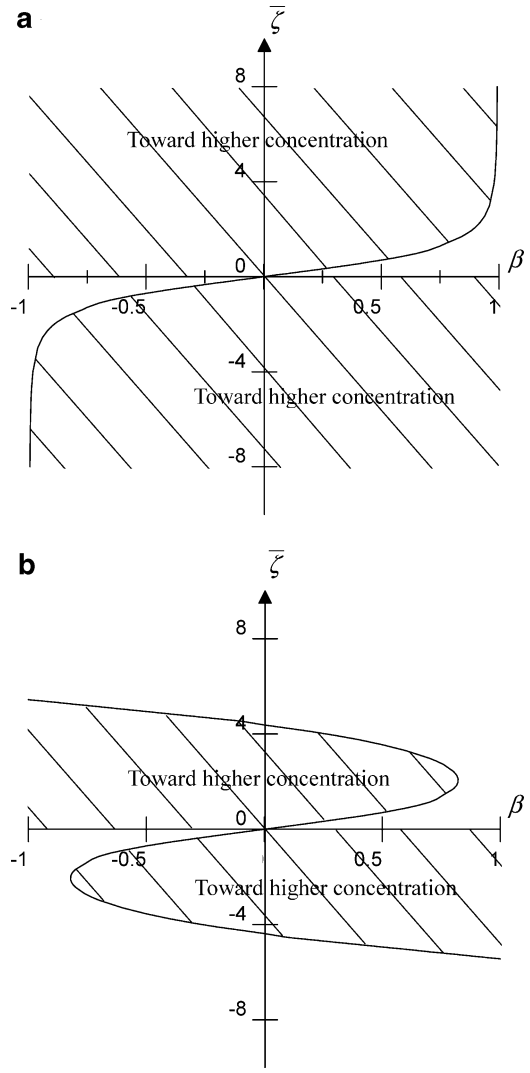


**Figure 8.** Maps showing the direction of the diffusioosmotic velocity at the axis of a capillary tube for the case of $\kappa R = 1$: (a) Pe = 0; (b) Pe = 1. The shadeless portion denotes flow toward lower electrolyte concentration.

When the value of Pe is finite, as indicated in Figure 8b, the probability of the diffusioosmotic flow of the electrolyte solution in the direction toward higher concentration for a combination of $\beta$ and $\bar{\zeta}$ is greatly reduced, due to the effect of the electrolyte convection. Again, this relaxation effect is very significant, irrespective of the thickness of the electric double layer adjacent to the capillary wall.

**5.5. Accuracy of the Approximation for the Potential Distribution.** Throughout this work we have adopted the mathematical approximation presented in section 2 for the solution of the electrostatic potential distribution on a cross section of the capillary tube. To check the accuracy of this approximation for the resulting diffusioosmotic velocity profile, in some typical cases, we numerically solve eqs 3 and 4 for $\bar{\psi}(r)$, curve fit its values in terms of a tenth-order polynomial, and then substitute it into eqs 18 and 26 to numerically determine the "exact" solution for the diffusioosmotic velocity $u(r)$.

Figure 9 gives a comparison of the approximate solution with the "exact" solution. It can be found that the difference between the two solutions for $u(r)$ increases with an increase in the normalized coordinate $r/R$ but is less than 5% if $r/R < 0.9$. This outcome means that the mathematical approximation presented in section 2 for the solution of $\bar{\psi}(r)$ is generally acceptable in the evaluation of the diffusioosmotic velocity of electrolyte solutions in a fine capillary tube, as it has been made in this work, when compared with the relevant experimental data.

## 6. Concluding Remarks

A theoretical study of the steady diffusioosmotic flow of solutions of symmetric electrolytes in a capillary tube is presented in this work. It is assumed that the fluid is only slightly nonuniform in the electrolyte concentration along the axial direction, but no assumption is made about the thickness of the electric double layer adjacent to the capillary wall. Both the effect of the radial distribution of the electrolyte ions (or of the electrostatic potential) and the effect of ionic convection caused by the diffusioosmotic flow itself (relaxation effect) on the axial electric field induced by the applied electrolyte concentration gradient are taken into account. The capillary wall may have either a constant surface potential or a constant surface charge density of an arbitrary quantity.

When the Poisson−Boltzmann equation in an approximate form and the modified Navier−Stokes equation applicable to the system are solved, the electrostatic potential distribution, the

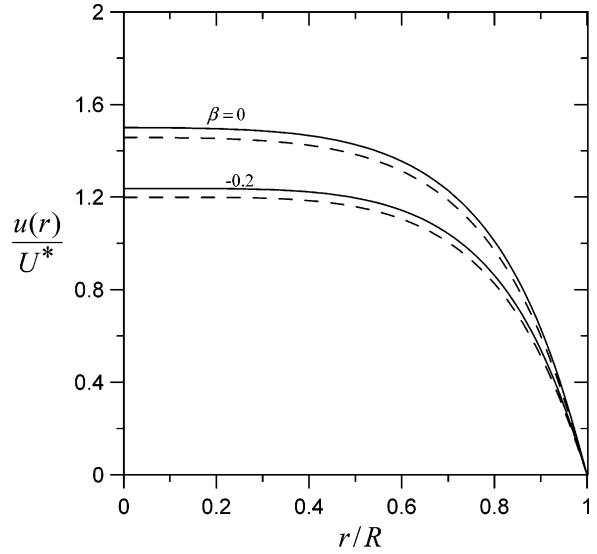


**Figure 9.** The normalized diffusioosmotic velocity distribution in a capillary tube for the case of $\bar{\zeta} = 6$, $\kappa R = 1$, and Pe = 1. The dashed curves represent the result obtained by using the mathematical approximation for the evaluation of $\bar{\psi}(r)$ in section 2 and the solid curves denote the numerical "exact" solution.

induced electric field distribution, and the dynamic pressure distribution under the influence of the imposed electrolyte gradient are determined either analytically or semianalytically. Numerical results for the local diffusioosmotic velocity on a cross section of the capillary tube as functions of relevant parameters are presented in detail. The results show that the effect of the deviation of the local induced tangential electric field inside the double layer from its bulk-phase quantity and the relaxation effect due to electrolyte convection are very important and cannot be neglected in the evaluation of the diffusioosmotic velocity of electrolyte solutions in the axial direction of the capillary tube, even for the case of a very thin double layer.

It is worth repeating that all the results in this study are obtained on the basis of a small external gradient of the electrolyte concentration in the axial direction of the capillary tube. If the imposed concentration gradient $|\nabla n^{\infty}|$ is relatively large, then the effect of variation of the electrostatic potential $\psi$ in the double layer adjacent to the capillary wall with the tangential position may not be neglected. However, it is reasonable for one to expect that this effect will lead to quantitatively rather than qualitatively different results.

A recent report[27] emphasizes that an electric double layer very often cannot be characterized only with a zeta potential, because there is an additional surface conductivity associated with the surface current caused by the external electric field within a thin layer between the particle surface and the slipping shear plane. When this surface conductivity effect is important, a modification of our analysis will be demanded.

**Acknowledgment.** This research was supported by the National Science Council of the Republic of China under Grant NSC95-2221-E-002-281.

LA062683N

(27) Dalgado, A. V.; Gonzalez-Caballero, F.; Hunter, R. J.; Koopal, L. K.; Lyklema, J. *Pure Appl. Chem.* **2005**, *77*, 1753.